Coastal Engineering 60 (2012) 326–333

Contents lists available at SciVerse ScienceDirect

Coastal Engineering

journal homepage: www.elsevier.com/locate/coastaleng

Short communication

Impact of a uniform bore on an erodible beach

Fangfang Zhu *, Nicholas Dodd, Riccardo Briganti

Infrastructure and Geomatics Division, Faculty of Engineering, University of Nottingham, Nottingham, NG7 2RD, England, UK

ARTICLE INFO

Article history:
Received 1 July 2011
Received in revised form 1 August 2011
Accepted 23 August 2011
Available online 28 September 2011

Keywords:
Swash
Sediment transport
Bore
Tsunami morphodynamics

ABSTRACT

The impact of a uniform bore on an erodible beach is investigated using a shallow water description and a sediment conservation equation. The solution, which is obtained using the method of characteristics, employs a cubic bed-load formula and a crudely calibrated sediment transport coefficient. It is found that, as with the fixed bed case of Hibberd and Peregrine (1979), a backwash bore forms, which for the mobile bed also comprises a bed step. It is found that this bed step achieves a significant height. The volume of sand deposited above the final still water level is consistent with that observed under certain events on some sandy beaches.

1. Introduction

The swash zone is a very dynamic and complex region on steeper beaches, in which waves collapse, run-up and run down the beach. Swash dynamics are of great significance to beach face evolution, and therefore are important to erosion/accretion at the shoreline, which is of prime importance to beach and coastal defence maintenance.

On steeper beaches waves frequently plunge or "collapse" on the beachface, as a wave or bore nears or reaches the shoreline (zero depth), leading to a swash event (run-up and backwash), with associated sediment movement.

Most studies of such swash events (flows) have made use of a shallow water description, in which the velocity is assumed depth-uniform and pressure hydrostatic, and this description is, overall, a good one.

There are some analytical shallow water solutions or approximations for the behaviour of a bore travelling to the shore, and climbing up the beach. Whitham(1958) used the method of characteristics with shock relations to provide an expression for the height of a bore as it propagates into still water (see also Keller et al., 1960). Shen and Meyer (1963) (hereafter SM63) derived an exact solution for the shoreline motion after bore collapse, and an approximate solution for the region close to the shoreline.

Peregrine and Williams(2001) (henceforth PW01) subsequently extended the SM63 solution to the whole swash by interpreting it as a dam-break problem on a sloping bed. This description has been used to examine swash dynamics by many researchers, and also to look at net erosion/deposition under a swash event (Pritchard and Hogg, 2005). Guard and Baldock(2007) pointed out that the PW01 solution is only a special case for the SM63 swash, and that it neglects the momentum behind the bore and therefore underestimates water depth in the lower- and mid-swash compared to experimental and numerical results.

A related but distinct description of bore-driven swash motion on a beach is that provided by Hibberd and Peregrine(1979) (hereafter HP79), who investigated numerically a uniform bore approaching a sloping beach. Here the bore separates two regions of constant water level, initially on constant depth; ultimately, the water level changes as the bore impacts on the beach. The deeper swash and the different accelerations on the constant and sloping parts result in the formation of a backwash bore. This finding confirmed the earlier prediction of Shen and Meyer(1963). Subsequently, Guard and Baldock(2007) also predicted the formation of a backwash bore in some special types of modified PW01 swash (essentially the same boundary conditions as those of HP79); Pritchard et al.(2008), who examined the same swash events as those in Guard and Baldock(2007) in analytical work, also predicted a secondary bore in both backwash and the uprush in long surf for certain types of swash events.

If an erodible bed is considered analytical solutions are more difficult to find. The dam-break problem on an initially flat bed is amenable to solution as a simple wave (see e.g. Kelly and Dodd, 2009), and therefore as an initial condition for the equivalent swash event (Kelly and Dodd, 2010). Kelly and Dodd(2010) (hereafter KD10) examined the morphodynamic equivalent of the PW01 solution, concluding, consistent with Pritchard and Hogg(2005), that net erosion occurs without consideration of suspended load.

As yet, the HP79 event has not been examined for an erodible beach. This type of event is potentially very interesting because if the backwash bore exists on an erodible beach it must be accompanied by a jump in bed level (via the shock relations: see KD10). Therefore, it seems possible that a so-called swash bar or berm might, in essence,

* Corresponding author.
E-mail address: evxfz2@nottingham.ac.uk (F. Zhu).

0378-3839
doi:10.1016/j.coastaleng.2011.08.006

be created by the backwash bore. Here we present a study to examine this issue. Furthermore, the HP79 event can be interpreted as an idealised tsunami impinging on a beach. Therefore, it can be used to obtain an estimate of the impact of a tsunami on a beach (see e.g. Young et al., 2010). Additionally, this case, if solved with sufficient accuracy, provides a solution for researchers to verify other shallow water morphodynamic solvers against (see also KD10). To this end we utilise the method of characteristics used by KD10 to achieve very high accuracy in the vicinity of shocks.

We briefly outline the model in the next section and present results thereafter, followed by conclusions. We present some verification tests in the appendix, including one against a state-of-the-art, finite difference morphodynamical code.

2. Model development

2.1. Governing equations

The nonlinear shallow water equations together with a bed-evolution equation are coupled to describe the morphodynamics in the swash zone:

$$\hat{h}_{\hat{t}} + \hat{u}\hat{h}_{\hat{x}} + \hat{h}\hat{u}_{\hat{x}} = 0 \tag{1}$$

$$\hat{u}_{\hat{t}} + \hat{u}\hat{u}_{\hat{x}} + g\hat{h}_{\hat{x}} + g\hat{B}_{\hat{x}} = 0 \tag{2}$$

$$\hat{B}_{\hat{t}} + \xi\hat{q}_{\hat{x}} = 0 \tag{3}$$

where $\hat{h}$ represents water depth (m), $\hat{u}$ is a depth-averaged horizontal velocity (ms^{-1}), $\hat{B}$ is the bed level (m), $\hat{q}$ is sediment flux (m^2s^{-1}), which is, in general, a function of $\hat{h}$ and $\hat{u}$, $\xi = \frac{1}{1-p}$ with p being bed porosity, and g is acceleration due to gravity (ms^{-2}).

Here, a simple but commonly used formula $q = A\hat{u}^3$ (see Grass, 1981) is employed for the bed load (see e.g. KD10), with A being the bed mobility parameter (s^2m^{-1}). So, Eq. (3) becomes:

$$\hat{B}_{\hat{t}} + 3\xi A\hat{u}^2\hat{u}_{\hat{x}} = 0 \tag{4}$$

All variables, except $\hat{t}$, g and ξ are defined in Fig. 1.

2.2. Non-dimensionalisation

To make the results more intercomparable, we non-dimensionalise all variables. Dimensionless variables are:

$$x = \frac{\hat{x}}{h_0}, t = \frac{\hat{t}}{h_0^{1/2}g^{-1/2}}, h = \frac{\hat{h}}{h_0}, u = \frac{\hat{u}}{(gh_0)^{1/2}}, B = \frac{\hat{B}}{h_0} \text{ and } q = \frac{\hat{q}}{q_0}, \tag{5}$$

where h_0 is a length scale, and q_0 represents a sediment flux scale, and $q_0 = A(gh_0)^{3/2}$ is chosen.

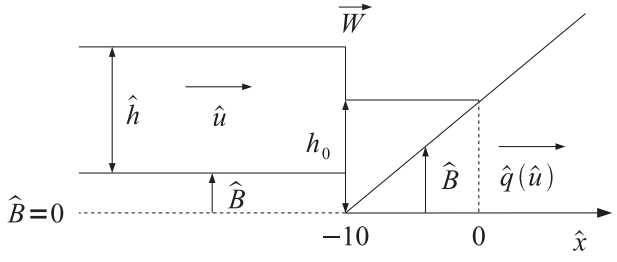

Fig. 1. Initial conditions for HP79 swash.

Substituting (5) into the governing Eqs. (1), (2) and (4) gives:

$$h_t + uh_x + hu_x = 0 \tag{6}$$

$$u_t + uu_x + h_x + B_x = 0 \tag{7}$$

$$B_t + 3\sigma u^2 u_x = 0 \tag{8}$$

where $\sigma = \xi Ag$. The equations are written in vector form:

$$\vec{U}_t + \mathbf{A}\left(\vec{U}\right)\vec{U}_x = 0 \tag{9}$$

with

$$\vec{U} = \begin{bmatrix} h \\ u \\ B \end{bmatrix}, \mathbf{A}\left(\vec{U}\right) = \begin{bmatrix} u & h & 0 \\ 1 & u & 1 \\ 0 & 3\sigma u^2 & 0 \end{bmatrix}.$$

The eigenvalues of **A** are the roots of the polynomial,

$$\lambda^3 - 2u\lambda^2 + \left(u^2 - 3\sigma u^2 - h\right)\lambda + 3\sigma u^3 = 0, \tag{10}$$

the roots of which may be denoted λ_1, λ_2 and λ_3, such that $\lambda_1 \le \lambda_3 \le \lambda_2$, and where $\sigma \to 0 \Rightarrow \lambda_3 \to 0$, $\lambda_1 \to u - \sqrt{h}$ and $\lambda_2 \to u + \sqrt{h}$. Thus, $\lambda_{1,2}$ can be said to correspond to hydrodynamic characteristics, and λ_3 to the speed of propagation of bed deformation.

2.3. Shock conditions

The morphodynamic shock conditions are:

$$h_R u_R - h_L u_L - (h_R - h_L)W = 0 \tag{11}$$

$$W(h_R u_R - h_L u_L) - \left(h_R u_R^2 + \frac{h_R^2}{2} - h_L u_L^2 - \frac{h_L^2}{2}\right) -$$

$$\frac{1}{2}(B_R - B_L)(h_L + h_R) = 0 \tag{12}$$

$$(B_R - B_L)W - \sigma\left(u_R^3 - u_L^3\right) = 0 \tag{13}$$

where the subscripts L and R denote the variables on the left side and right side, respectively, and W is the shock speed. See KD10 for more details.

2.4. Numerical method

The method of characteristics has the advantage of high accuracy at shocks (e.g. backwash bore). Here we follow Kelly and Dodd (2010), in using the Specified Time Interval Method Of Characteristics (STI MOC) (see also Kelly and Dodd, 2009), with the one amendment that we implement second order accuracy in interpolation. This is used to solve Eqs. (6), (7) and (8) simultaneously. Details of this numerical method are given in Kelly and Dodd(2009) and KD10.

2.5. Initial and boundary conditions

2.5.1. Initial conditions

The initial conditions are shown in Fig. 1. In the region of $x \le -10$ the bed is flat while for $x \ge -10$ the beach is of a uniform slope, with the beach slope $\alpha = 0.1$. At $t = 0$, there is a bore of height 0.6 propagating towards the beach and located at $x = -10$; there is therefore a discontinuity in h, u and B at $x = -10$, separating left (L) and right (R) regions. For $x \ge -10$, $h(x) = 1 - \alpha(x + 10)$, $u(x) = 0$ and $B(x) = \alpha(x + 10)$ (conditions immediately to the right of the initial discontinuity are therefore $U_R = 0$, $h_R = 1$, and $B_R = 0$). The initial

shoreline position is at $x=0$. At $t=0$ $x\leq -10$ is a constant region such that $h(x)=h_L$, $u(x)=u_L$ and $B(x)=B_L$, where $h_L=1.6$ and such that u_L and B_L are determined by shock relations (11)-(13).

2.5.2. Boundary conditions

The seaward boundary is chosen so as to be far enough away from the shore that h, u and B at that point are uninfluenced by the wave reflected from the shore throughout the computation time. Here the seaward boundary is at $x=-100$, and $h(-100,\ t)=h_L$, $u(-100,\ t)=u_L$ and $B(-100,\ t)=B_L$. The landward boundary is a wet–dry boundary.

3. Results

The complete solution for $\sigma=0.0654$ (this value being chosen for consistency with KD10, who determined it by crudely equating it to field measurements) for a uniform bore on an erodible bed is shown in Fig. 2.

Note that i) run-up is significantly reduced compared to that observed by Hibberd and Peregrine(1979), consistent with the results of KD10; ii) the event results in deposition from $x\approx 4.57$ almost to the maximum run-up position, x_{smax}, and erosion occurs mainly in the region $-10<x<4.57$ (see Fig. 2(c)); and iii) a morphodynamic backwash bore is formed at $(x,\ t)\approx(13.57,\ 47.09)$. This shock is formed by the convergence of bed (i.e. λ_3 (KD10)) characteristics. This backwash bore ultimately results in a bed-step being created on the beach.

The bed profile at $t=54.68$, (when $u(x_s)=0$, and after which time the water level advances again slightly) is shown in Fig. 3. As previously mentioned that there is an overall deposition in the swash zone, and erosion mainly occurs in the region $-10<x<4.57$. It should be noted the swash cycle is not finished and the bed will change further, albeit by only a small amount.

The resulting final beach profiles and changes in the swash zone are shown for a series of σ in Fig. 4.

The bed-step height and crest elevation are shown in Fig. 5 for various σ. Note that bed-step crest elevation here refers to the vertical distance from the top of the bed step in the final profile to the original bed level at that location ($x=12.69$ for $\sigma=0.0654$). As the bed becomes less mobile the bed-step height decreases, as might be expected. However, the bed-step height (one measure of the shock strength) eventually decreases with increasing σ, as the point of inception of the backwash bore is delayed because of the changed dynamics of the mobile bed: see Fig. 6. The bed-step crest elevation, however, increases with mobility as more sediment is deposited in the swash.

Note, in particular, the velocities (Fig. 2(b)). In the uprush the maximum velocity ≈ 0.76 times that for the fixed bed (cf. Fig. 9). The peak velocity in the backwash ≈ 0.58 times the fixed bed equivalent. This discrepancy results from the smaller run-up and the reduced slope for

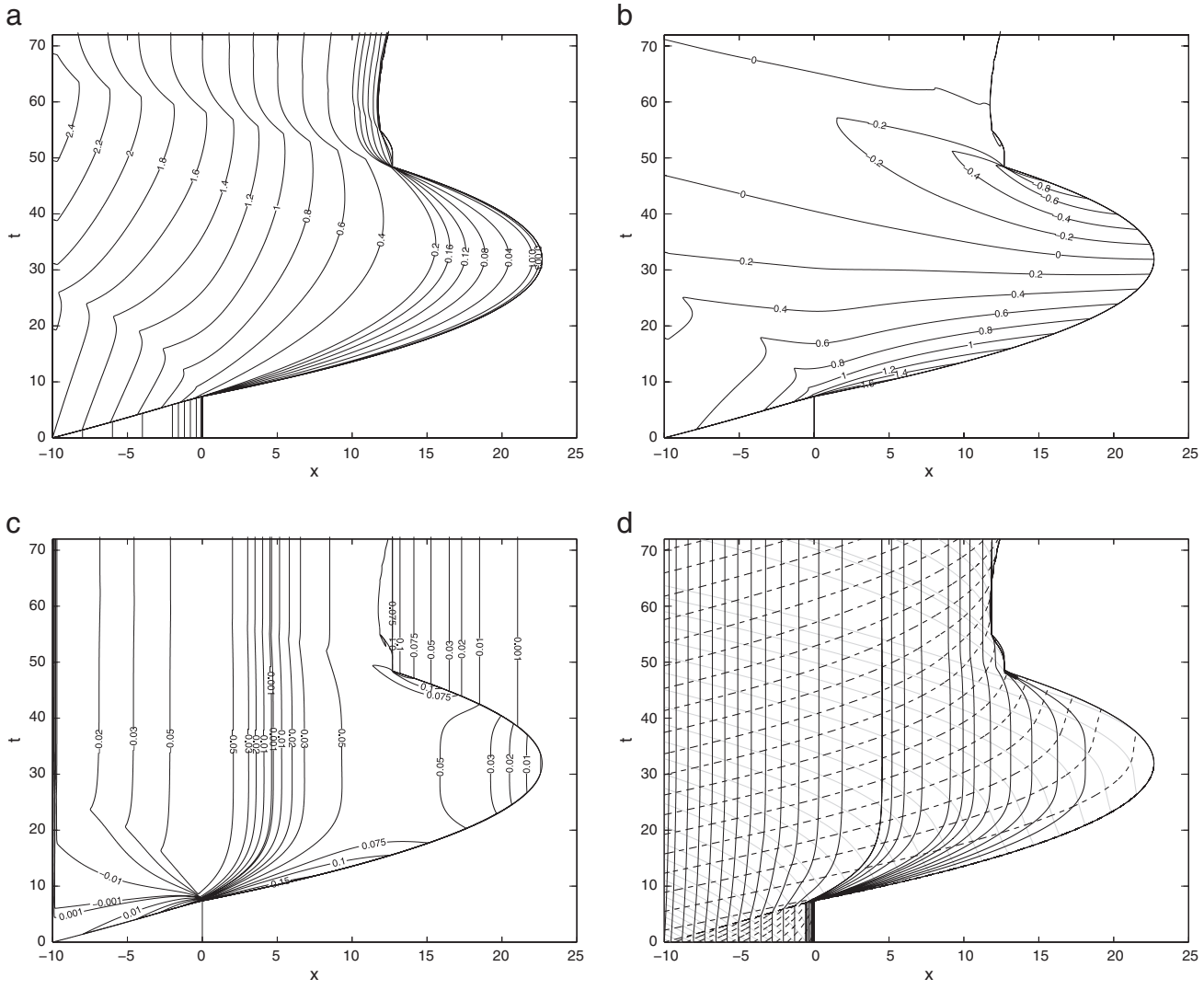

Fig. 2. The mobile bed HP79 event ($\sigma=0.0654$). (a) h; (b) u; (c) change in bed elevation, $\Delta B=B-B(x,t=0)$; (d) characteristics diagram (λ_3 characteristics denoted by solid, black lines).

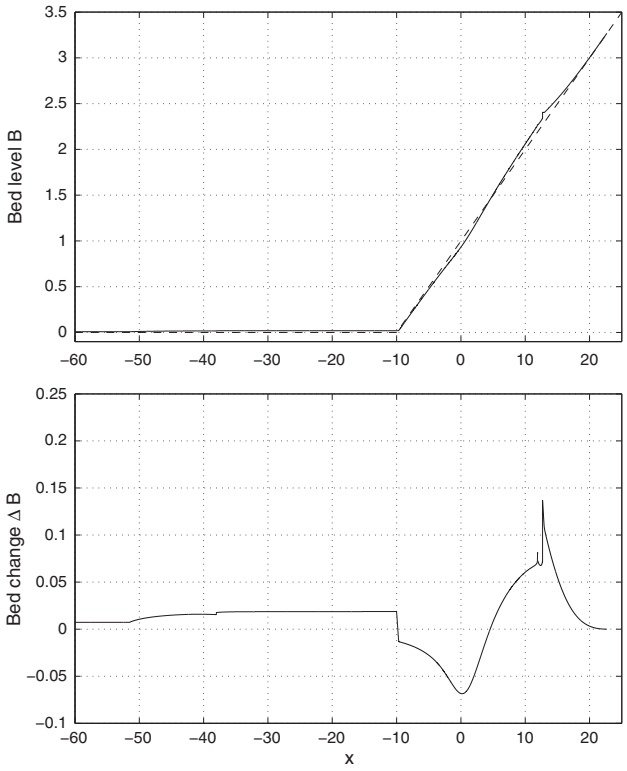

Fig. 3. Dimensionless bed profile (top) and bed change (bottom) at $t = 54.68$ for mobile bed HP79 event ($\sigma = 0.0654$).

the backwash (because of the deposition: see Fig. 2(c)). This results in a weaker shock that forms later in the swash event. The shock strengths (i.e. the change in λ_3 across the shock: $\lambda_R - \lambda_L$, where R and L refer to

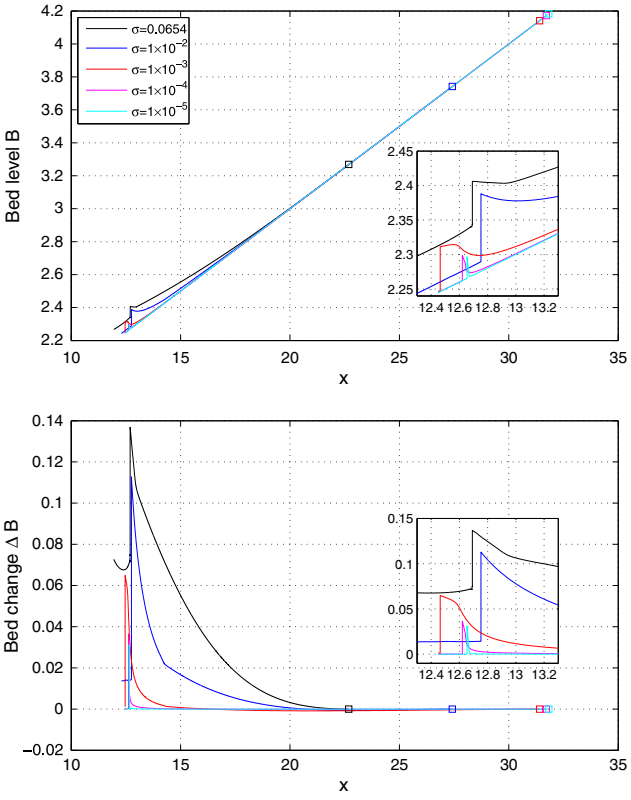

Fig. 4. Dimensionless final bed profile (top) and bed change (bottom) for various σ for mobile bed HP79 event. Position of maximum run-up depicted by □.

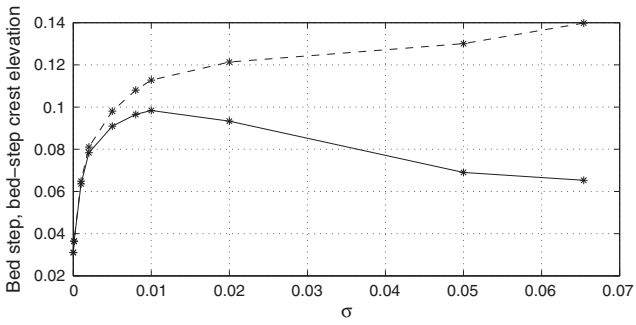

Fig. 5. Dimensionless bed-step height (solid line) and bed-step crest elevation (dashed line) for various σ for mobile bed HP79 event.

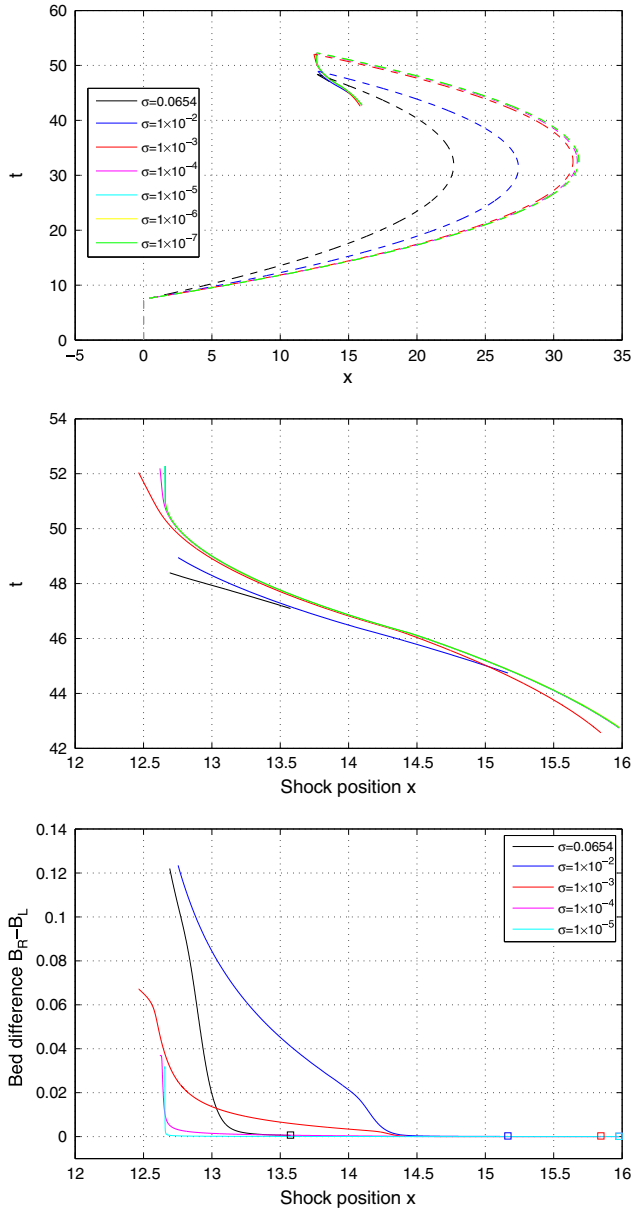

Fig. 6. Dimensionless backwash bore position and shoreline position (top); and blow-up of backwash bore position (middle). Bed-step height as a function of shock position (bottom) throughout the swash event. □ indicates point of shock inception. All for various σ values for mobile bed HP79 event.

values on the right and left of the shock) can be seen in Fig. 7 for various σ.

The smaller run-up also leads to reduced flow velocities at the tip. It is the flow velocity at the tip that determines how much the bed elevation decreases as the shoreline recedes, so although increased bed mobility would seem to favour a larger bed-step in principle, the changed dynamics lead eventually to a decreasing bed step.

It should be noted that in Fig. 6, for very small σ the bed difference across the shock remains extremely small even when the shock is considerably developed (see Fig. 7). From the shock condition (13), we have $B_R - B_L = \sigma(u_R^3 - u_L^3)/W$, so that when $W \to 0$, the bed difference $B_R - B_L$ grows substantially. Further, as W is extremely small, the shock moves very little, so the large $B_R - B_L$ is confined to a region of small width, which also explains why the large bed level increase in the final bed profile for small σ in Fig. 4 (i.e., the bed-step) is confined to a region of small width.

4. Concluding remarks

The HP79 uniform bore is examined on a mobile bed. Similar to the fixed bed simulation of Hibberd and Peregrine(1979) a backwash bore is formed, which is, however, less pronounced and forms later in the backwash: see Fig. 6. However, on an erodible beach the backwash bore is associated with the formation of a beach step (or swash bar). If we insert dimensional quantities typical of the swash into the solution (for $\sigma = 0.0654$), we find that for $h_0 = 1$ m (and therefore initial bore height $= 0.6$ m) the resulting beach step is 0.062 m high, and the amount of sediment deposited in the region $x > 0$ (at $t = 54.68$) is 1325.74 kg/m. This region might be considered the original swash zone. Due to the change in the water level in the HP79 event, however, the region $x > 11.95$ might also be considered the swash region. In that case (also for $t = 54.68$) the overall deposition is 968.09 kg/m.

These figures are larger than but of a similar order of magnitude to the large depositional events observed by Blenkinsopp et al.(2011), who observed bed changes of up to 0.043 m and maximum net fluxes of hundreds of kg/m over one swash event. The HP79 mobile bed event inevitably gives overall deposition because the water level is raised. This can, however, be interpreted as a long period bore, in which free surface elevation decreases relatively slowly in lee of the bore front (shock). This type of event could provide large deposition in the swash.

Turning now to the case of a tsunami impinging on the same beach, if we take $h_0 = 5$ m (and therefore a tsunami height of 3 m on 5 m depth) we find that the deposits are about 11 cm thick on an average in the "swash" zone (a maximum change of 31 cm), which extends a distance of 113 m. This is in accordance with the suggestion of Morton et al. (2007) that tsunami deposits are generally less than 25 cm thick, extending hundreds of metres inshore.

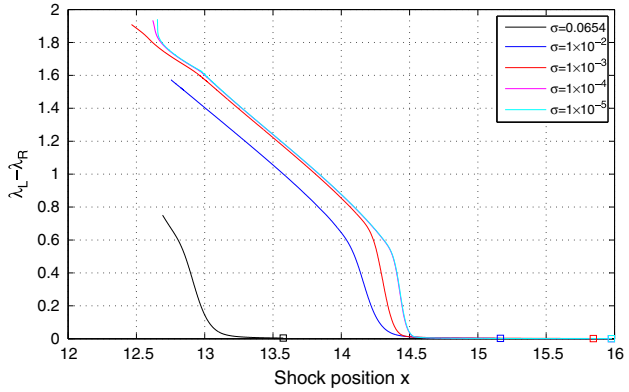

Fig. 7. Dimensionless shock strength as a function of shock position for various σ for mobile bed HP79 event. □ indicates point of shock inception.

Acknowledgements

FZ and ND would like to express their gratitude to the International Office of The University of Nottingham, and to the China Scholarship Council for providing financial support. RB would like to express his gratitude to the EPSRC for supporting him through a Career Acceleration Fellowship (EP/I004505/1).

Appendix A. Verification of model

Three comparisons are made to verify the model. First, we compare with the PW01 analytical solution, which gives us a clear idea of the accuracy of the model. Note that PW01 is a non-erodible bed solution; we approximate it here by putting $\sigma = 1 \times 10^{-7}$. We then compare with the original HP79 swash event (again with $\sigma = 1 \times 10^{-7}$). Of particular importance here is the correct formation of the backwash bore. We then compare with the PW01 swash event over a mobile bed ($\sigma = 0.0654$), namely the numerical solution of KD10. This allows confirmation that the code works correctly morphodynamically.

Appendix A.1. PW01 swash event ($\sigma = 1 \times 10^{-7}$)

We use $\Delta x = 2.5 \times 10^{-3}$ and $\Delta t = 4 \times 10^{-4}$. The comparison is shown in Fig. 8. The maximum run-up shows a discrepancy of 0.56%.

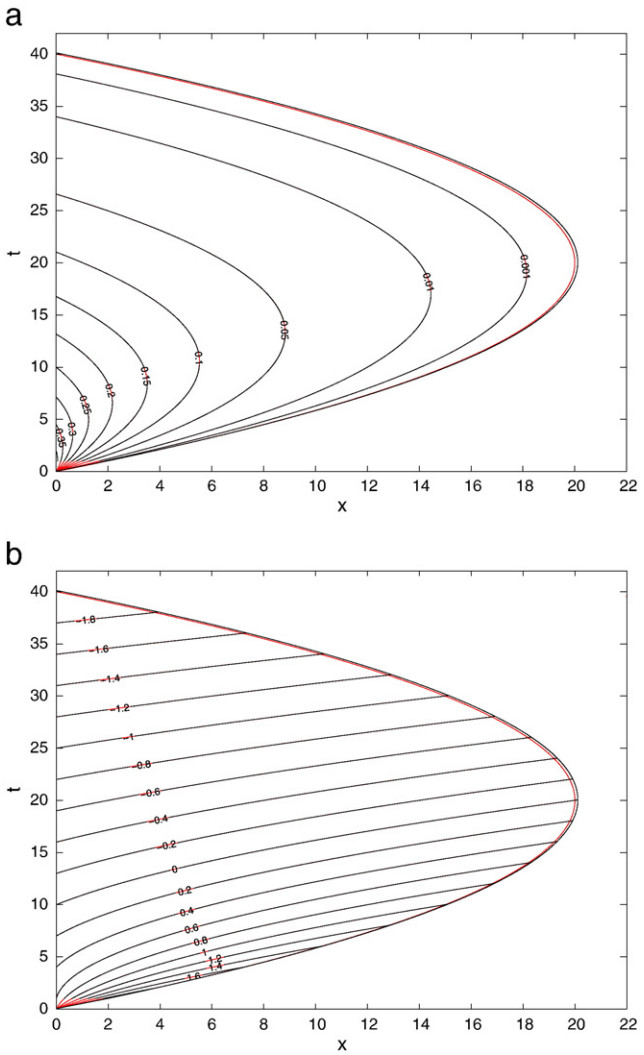

Fig. 8. Comparison with PW01 solution ($\sigma = 1 \times 10^{-7}$). (a) h; (b) u. Black: present model. Red: PW01 analytical solution.

The numerical scheme therefore slightly overpredicts the maximum run-up.

Appendix A.2. HP79 swash event ($\sigma = 1\times10^{-7}$)

In this simulation $\Delta x = 5\times10^{-3}$ and $\Delta t = 2\times10^{-3}$ are used. The maximum run-up predicted by the model is slightly bigger than that of Hibberd and Peregrine (1979): see Fig. 9 and also the comment in the preceding section. Another possible reason for this is that $h(x = x_s) \equiv 0$ in our model, while that in Hibberd and Peregrine (1979) is 1×10^{-4}; note that the contour $h = 1\times10^{-4}$ for the present model in Fig. 9(a) is quite close to the shoreline of HP79. It should also be borne in mind that the pioneering work of HP79 utilised a complicated shoreline condition that is not usually used in modern codes (see also Briganti and Dodd, 2009). The u comparison is shown in Fig. 9(b). The largest discrepancies are in h, particularly around the backwash bore. The shock resolution in the present model is probably more accurate than that in HP79. Lastly, it should also be borne in mind that the results from HP79 were here transcribed for comparison purposes by scanning the original figure into a CAD package and then manually adding contour points that were then converted to (x, t) coordinates.

Appendix A.3. KD10 swash event ($\sigma = 0.0654$)

In this simulation $\Delta x = 1\times10^{-2}$ and $\Delta t = 2\times10^{-3}$ are used. The comparison is shown in Fig. 10.

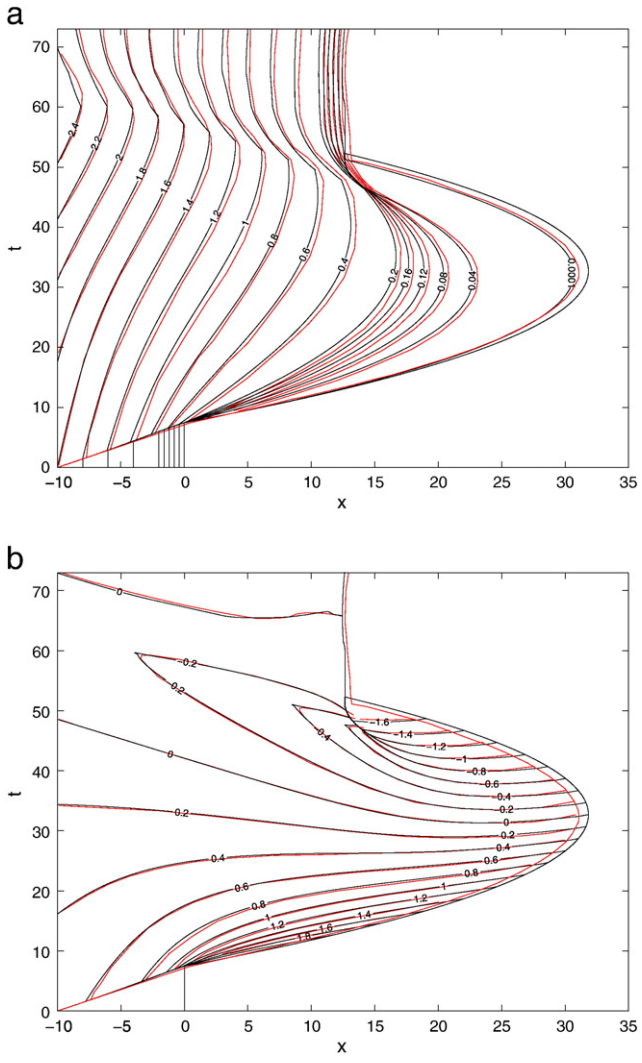

Fig. 9. Comparison with HP79 solution (i.e. present model for $\sigma = 1\times10^{-7}$). (a) h; (b) u. Black: present model. Red: HP79 numerical solution.

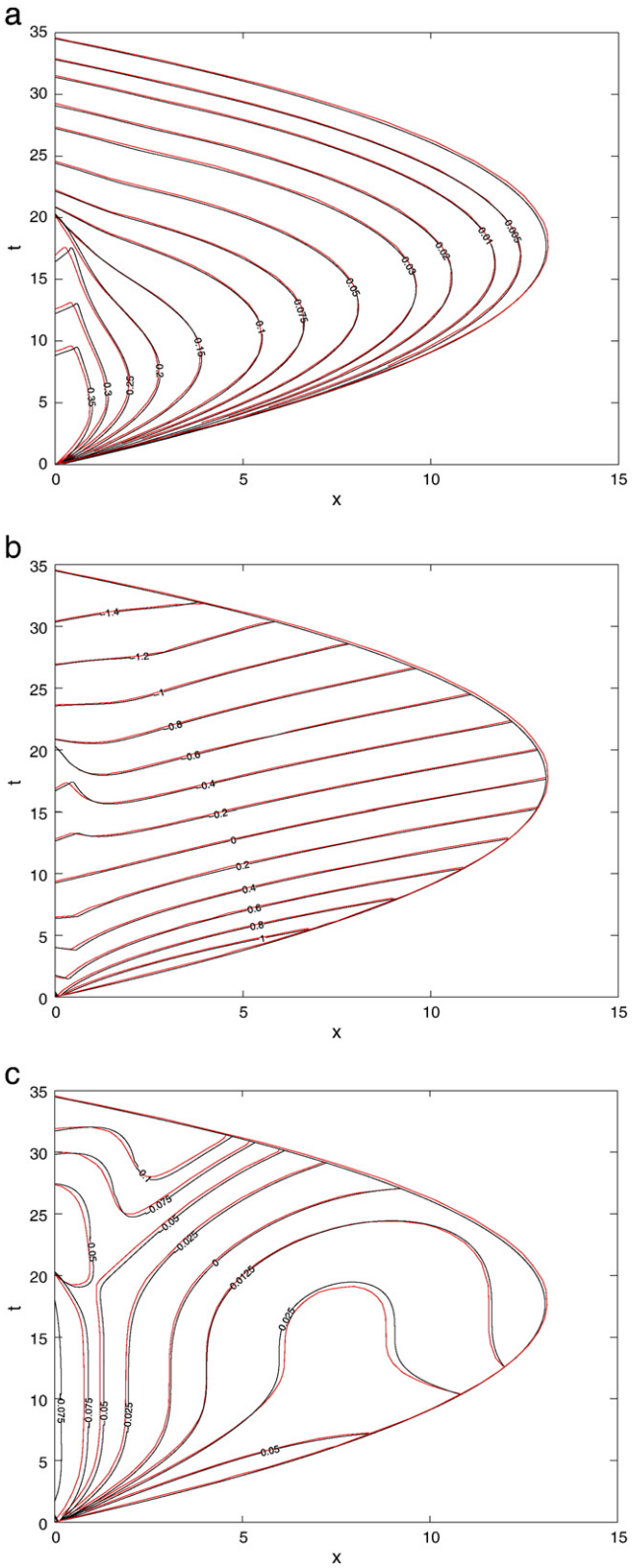

Fig. 10. Comparison with KD10 solution ($\sigma = 0.0654$). (a) h; (b) u; (c) ΔB. Black: present model. Red: KD10 numerical solution.

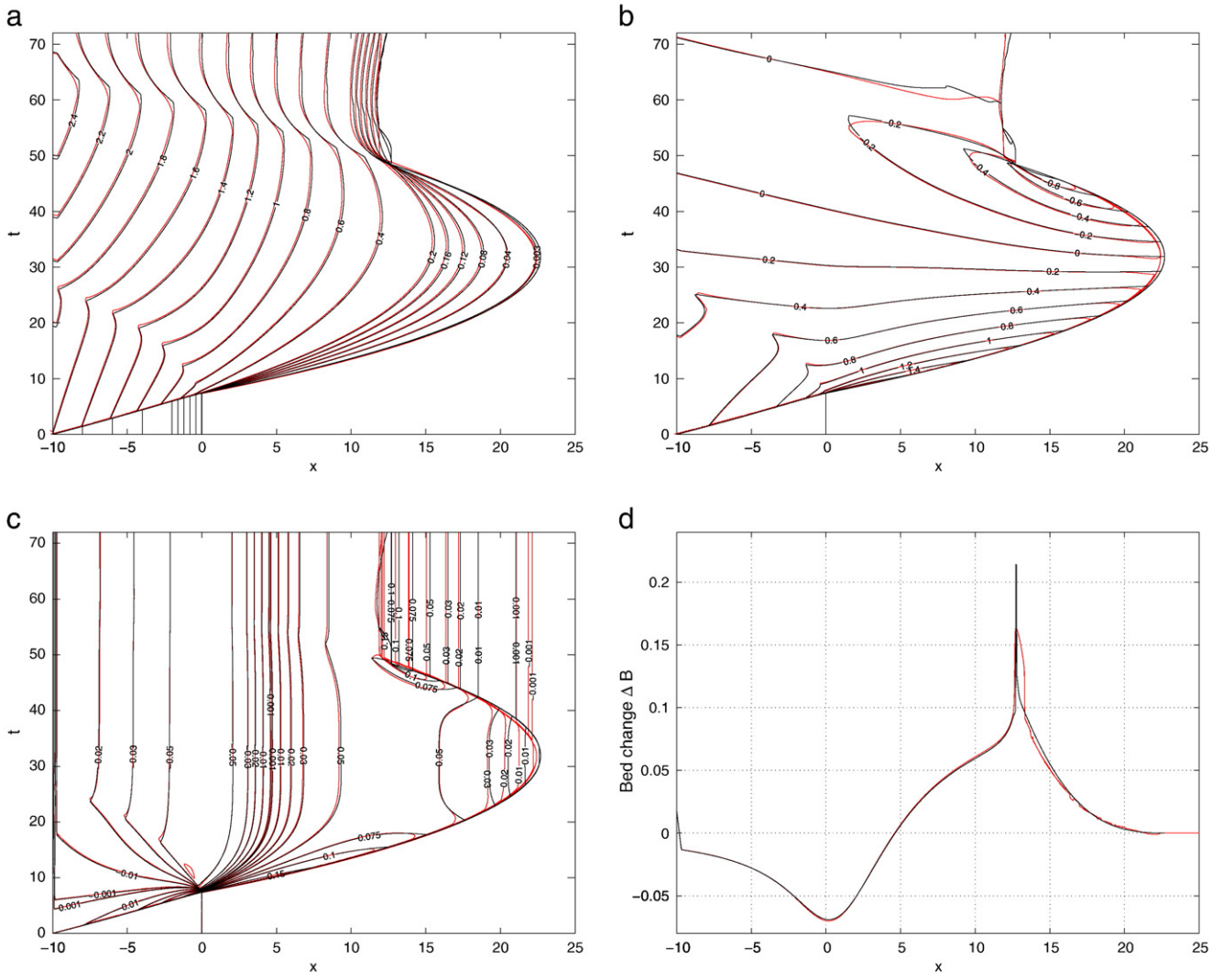

Fig. 11. Comparison using mobile bed HP79 event ($\sigma = 0.0654$) with Briganti et al. (2011). (a) h; (b) u; (c) ΔB. (d) Bed change (ΔB) at the point of bed-step formation ($t = 48.4$). Black: present model. Red: Numerical solution using model of Briganti et al. (2011).

Only small discrepancies are found in contours for h and u, while there are larger discrepancies in that for ΔB. As mentioned, the present scheme uses the method of KD10, except for second order spatial accuracy being implemented.

Appendix B. Comparison against state-of-the-art morphodynamic solver for HP79 swash event ($\sigma = 0.0654$)

In this simulation $\Delta x = 1 \times 10^{-2}$ and $\Delta t = 2 \times 10^{-3}$. The HP79 mobile bed swash event is considered again but comparison is made with the finite difference model of Briganti et al. (2011): see Fig. 11. The purpose is to examine the degree of correspondence that may be expected of the solution presented with engineering codes. Note that the model of Briganti et al. (2011) is run with $\Delta x = 0.01$, a minimum depth of 0.003, and a Courant number of 0.45.

There is one backwash bore in the simulation with the STI MOC method, while it is more difficult to say for certain when a bore occurs in the model of Briganti et al. (2011). Furthermore, there are clear discrepancies at the point of bed-step formation (see Fig. 11(d)). These discrepancies are not, however, surprising since shock-capturing codes will smear shocks to some degree (because they strike a balance between high accuracy and the requirement for no numerical oscillations to be present), and because at the moving shoreline very high accuracy is difficult to achieve (see Briganti and Dodd, 2009); and at the point of bed-step formation a shock and a shoreline coalesce.

Notwithstanding these discrepancies, the agreement in the final bed level, which is more difficult to predict than u and h, is remarkably good over most of the domain, and provides some reassurance that coastal engineering codes will be able to reproduce most of this process to a high degree of accuracy. Note also that the results from the model of Briganti et al. (2011) are unfiltered and unaveraged, and so exhibit small jumps in ΔB in the swash region, which sometimes occur during wetting and drying.

References

Blenkinsopp, C.E., Turner, I.L., Masselink, G., Russell, P.E., 2011. Swash zone sediment fluxes: field observations. Coastal Engineering 58, 28–44.
Briganti, R., Dodd, N., 2009. Shoreline motion in nonlinear shallow water coastal models. Coastal Engineering 56 (5–6), 495–505.
Briganti, R., Dodd, N., Kelly, D.M., Pokrajac, D., 2011. An efficient and flexible solver for the simulation of the morphodynamics of fast evolving flows on coarse sediment beaches. Int. J. Numerical Meth. Fluids. doi:10.1002/fld.2618.
Grass, A., 1981. Sediment transport by waves and currents. Technical Report FL29. University College London, London Centre for Marine Technology.
Guard, P.A., Baldock, T.E., 2007. The influence of seaward boundary conditions on swash zone hydrodynamics. Coastal Engineering 54, 321–331.
Hibberd, S., Peregrine, D.H., 1979. Surf and run-up on a beach: a uniform bore. Journal of Fluid Mechanics 95, 323–345.

Keller, H., Levine, D.A., Whitham, G.B., 1960. Motion of a bore over a sloping beach. Journal of Fluid Mechanics 7, 302–316.
Kelly, D.M., Dodd, N., 2009. Floating grid characteristics method for unsteady flow over a mobile bed. Computers and Fluids 38, 899–909.
Kelly, D.M., Dodd, N., 2010. Beach face evolution in the swash zone. Journal of Fluid Mechanics 661, 316–340.
Morton, R.A., Gelfenbaum, G., Jaffe, B.E., 2007. Physical criteria for distinguishing sandy tsunami and storm deposits using modern examples. Sedimentary Geology 200, 184–207.
Peregrine, D.H., Williams, S.M., 2001. Swash overtopping a truncated beach. Journal of Fluid Mechanics 440, 391–399.
Pritchard, D., Hogg, A.J., 2005. On the transport of suspended sediment by a swash event on a plane beach. Coastal Engineering 52, 1–23.
Pritchard, D., Guard, P.A., Baldock, T.E., 2008. An analytical model for bore-driven run-up. Journal of Fluid Mechanics 610, 183–193.
Shen, M.C., Meyer, R.E., 1963. Climb of a bore on a beach. Part 3. Run-up. Journal of Fluid Mechanics 16, 113–125.
Whitham, G.B., 1958. On the propagation of shock waves through regions of non-uniform area or flow. Journal of Fluid Mechanics 4, 337–360.
Young, Y.L., Xiao, H., Maddux, T., 2010. Hydro- and morphodynamic modeling of breaking solitary waves over a fine sand beach. Part 1: experimental Study. Marine Geology 269, 107–118.